PROCEEDINGS, 41st Workshop on Geothermal Reservoir Engineering
Stanford University, Stanford, California, February 22-24, 2016
SGP-TR-209

Hydrothermal Alteration of the Hidden Granite in the Geothermal Context of the Upper Rhine Graben

Jeanne Vidal[1], Marc Ulrich[1], Hubert Whitechurch[1], Albert Genter[2], Jean Schmittbuhl[1], Eléonore Dalmais[2], Violaine Girard-Berthet[1]

[1]EOST, University of Strasbourg, 5 rue René Descartes, 67000 Strasbourg, France

[2]ES-Géothermie, 3A chemin du Gaz, 67500 Haguenau, France

j.vidal@unistra.fr

Keywords: *hydrothermal alteration, sediment-basement interface, Soultz-sous-Forêts, , Upper Rhine Graben*

ABSTRACT

The sedimentary cover of the Upper Rhine Graben (URG) is locally characterized by a thermal gradient up to 100 K/km like in Soultz-sous-Forêts or Rittershoffen (France). This high thermal gradient decreases to 5 K/km at the sediment- *Rittershoffen* basement interface due to hydrothermal convective cells that circulate inside a nearly vertical fracture network affecting both the granite basement and the Triassic sediments above it. Therefore the sediment-basement interface is very challenging because the high thermal flux is attractive for geothermal exploitation. However natural permeability, evidenced by brine circulation, was only observed when the well cross-cuts a Hydrothermally Altered Fractured Zone in the deep Paleozoic granite. The uppermost top section of the granite was affected by a paleo-weathering superimposed alteration and is highly fractured but permeability evidence of this section was never clearly observed during drilling operations. In order to explain the permeability behaviour of fracture at the top of the basement, a detailed mineralogical investigation was carried out. Thin sections from a fully core Soultz well, EPS-1, were observed and analysed by several in situ technics including electron microprobe, SEM and LA-ICP-MS. Chemical maps were also acquired by SEM and treated based on a new routine, specially developed Matlab©-based code, in order to identify mineral phase relationships. The results show that secondary quartz, carbonates and illite observed in the fracture network in the granite derive from multiple processes of dissolution-precipitation after hydrothermal fluid events linked to the granitic basement geological history. The formation of secondary phyllosilicates and carbonates leads to a significant gain in volume that may reduce the porosity. Based on the mineralogical observations, it is proposed that the successive hydrothermal and paleo-weathering events characterized with dissolution-precipitation cycles tend to reduce fracture/matrix permeability of the uppermost granitic basement.

1. INTRODUCTION

The thermal regime of the Upper Rhine Graben (URG) is characterized by a series of geothermal anomalies near Soultz-sous-Forêts (Alsace, France), Rittershoffen (Alsace, France) and Landau (Rhine-Palatinate, Germany). These areas reveal local thermal gradients up to 100 K/km in the uppermost part of the sedimentary cover attributed to hydrothermal convective cells circulating inside a nearly vertical fracture network in the granite basement and in the Triassic fractured sediments above it (Schellschmidt, 1996; Pribnow and Schellschmidt, 2000). The thermal gradient decreases slowly to 5 K/km at the sediment-basement interface. The top of the basement is thermally attractive but its hydraulic behaviour is fracture dependent. Detailed structural studies on 800 m length of continuous EPS-1 core (Soultz) on Paleozoic monzogranite showed a higher average fracture density at the top of the granite due to the superimposition of sub-vertical fractures with nearly horizontal joints (Genter et Traineau, 1996). About six Soultz wells penetrated the uppermost granite section but any of them clearly shown some evidences of residual permeability during drilling operations. Residual permeability in the granite is intimately linked to Hydrothermally Altered Fractured Zones (HAFZ) showing a cluster organization deeper in the granitic basement.

In the framework of the geothermal exploration, the study of alteration at the top of the granitic basement could aim to better understand its hydraulic behaviour characterized with permeability variations. It also contributes to identify the geological factors that could impact the thermal profile such as the natural radioactivity distribution in the top basement.

For that, the study presents accurate investigations of the minerals that fill fractures at the top of the basement in EPS-1. Multiple technics include Scanning Electron Microscope (SEM) acquisition, electron microprobe and LA-ICP-MS measurements have been performed on thin sections of fractures. Results about secondary mineral phases fill fractures and their spatial relationships are correlated with geophysical well logging data interpretation and expanded to the Rittershoffen geothermal site. Final goal is to link the mineralogy of the fractures and their relative chronology of crystallization to the major tectonic events and fluid circulations in this part of the Upper Rhine Graben.

2. GEOLOGICAL SETTINGS

2.1 Alteration of the Soultz granite

In 1990, the old petroleum well EPS-1 is deepened to 2227 m depth MD and full cored for seismic purpose. The well penetrates the granitic basement at 1418 m depth. The deep granite is considered as an Mg-K monzogranite (Figure 1) (Stussi et al, 2002). The granite is composed by quartz, biotite, hornblende, K-feldspar, plagioclase and accessory minerals (magnetite, titanite and apatite). It is a very

radioactive granite with U content of 10 ppm vs 4 ppm for a standard granite of the Vosges area and Th content of 27 ppm vs 15 ppm for a standard granite. The granite batholith was affected by a pervasive alteration during its emplacement that involves the alteration of plagioclase and biotite and subsequent formations of corrensite and chlorite (Genter, 1989). Then the batholith has been affected by fracture event, which caused the formation of large sets of fractured zones. They represent the main pathways for circulating fluids. The subsequent hydrothermal alteration superimposes the pervasive one and significantly changed the granite mineralogy. In the matrix, corrensite and chlorite are transformed into illite (Genter, 1989). K-feldspars are also transformed into illite when brittle deformation is developed. Primary plagioclases react with rich CO_2 fluid circulating into the fractured granite and carbonates crystallize into matrix and fractured zone. All these reactions are accompanied by the formation of secondary quartz.

From 1418 to 1550 m depth, the granite is affected by paleo-weathering responsible for the whole reddish color (Fe-oxides) of the top of the granitic basement. The paleo-weathering is a consequence of the paleo-emersion of the top of the granitic basement. During this period, magnetic minerals as magnetite are altered into Fe-oxides or Fe-hydroxides minerals. The matrix of the granite is highly transformed into illite with some rare K-feldspars. The uplift of the top basement involves a decompression of the rock masse and the formation of horizontal fractures called jointing. Fractures at the top basement are filled by quartz, illite, carbonates and iron oxides as hematite.

The post-Variscan tectonic events of the Upper Rhine Graben such as diagenesis, subsidence, extension or reactivation of Hercynian structures are characterized by successive hydrothermal fluid circulations. During these more recent circulations (Permian, Jurassic, Cretaceous and even younger times), illite crystallise in both veins and matrix (Schleicher et al., 2006). Ferromagnesian mineral and feldspars transformations occurred after fluid circulations. Carbonates and quartz veins precipitate and grow. The relative chronology of alteration and mineralogical transformation is not trivial because several hydrothermal circulation events took place in during the geological and tectonic history of this Paleozoic granite, which emplaces 333 M years ago (Cocherie et al, 2004). This study is focused on the major vein alteration at the top of the granite.

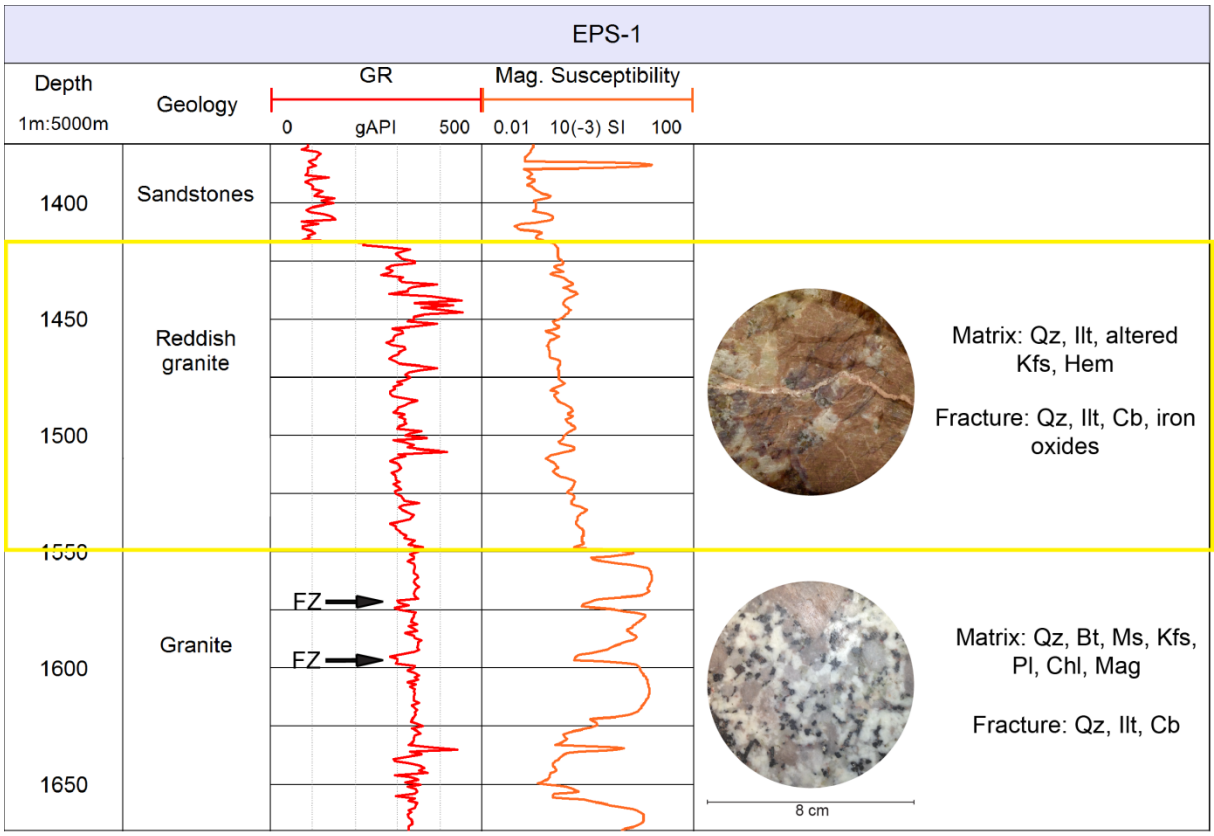

Figure 1: Gamma Ray and magnetic susceptibility in the well EPS-1 with core pictures of reddish granite and Mg-K granite (FZ = fractured zone, yellow frame = zone of the study, Qz=Quartz, Bt=Biotite, Ms=Muscovite, Kfs=K-feldspars, Pl=Plagioclase, Chl=Chlorite, Mag=Magnetite)

The granite alterations are observed macroscopically on core samples with the mineralogy but also with well-logging data. The Gamma Ray (GR) is the study of the natural radioactivity into the well. The sediment-basement interface is evidenced by a large positive variation (from 70 to 225 gAPI) that indicates the transition to the radioactive granite. In the reddish granite section, the natural radioactivity varies from 225 to 450 gAPI while in the deep granite amplitudes of variations are more restrained (from 300 to 350 gAPI) excepted for sharp positive peaks that can reach more than 600 gAPI. The magnetic susceptibility is about 12.5 SI in the granite. In the reddish granite, it decreases to 0.4 SI that indicates the leaching of primary magnetic and ferromagnesian minerals (magnetite, biotite

and hornblende) due to the superimposition of hydrothermal fluid alteration events. The important radioactivity at the top of the basement could influence the thermal flux.

2.2 Fractures in EPS-1 well

The borehole locally cross cuts fractured zones. They are evidenced by well-logging variations like the a negative anomaly of GR and magnetic susceptibility that correlate at 1570 m depth and 1670 m depth. These fractured zones could be pathways for paleo-circulation and primary minerals were dissolved (Figure 1). These fractures zones are also seen on core samples. Some of the fractures cross-cutting by the borehole showed a natural permeability during drilling operations and are called HAFZ. These zones combined a high fracture density and a strong hydrothermal alteration with successive dissolution-precipitation of primary minerals. At Soultz, HAFZ occurred in the deep granite where the fracture density is 3.2 fract/m whereas it is 7.6 fract/m at the top of the granite (Genter and Traineau, 1996).

The fracture fillings present the same mineralogy in the whole granitic basement but the proportion of minerals varies according to the granite petrography (Figure 2) (Genter and Traineau, 1996). Hematite is mainly concentrated at the top granitic basement into fractures in Mode I (jointing and tension fractures), whereas illite is more concentrated into fractures in Mode II (shearing) from Mg-K monzogranite. Carbonates are almost exclusively present into fractures in Mode I and the number of fractures filled by carbonates increases with depth. Quartz is present in the whole granite in fractures in both Mode I and Mode II. Study of quartz vein into EPS-1 show at least seven generations of quartz (Smith et al., 1998). Primary quartz occurs as clasts and angular fragments while secondary quartz is microcrystalline. Fluid inclusion analyses indicate that they precipitate after several pulse of hot water whose the salinity and the chemical composition vary. Recent generations of quartz crystallize at the modern fluid temperature (150°C) and pressure (200°C) suggesting that quartz veins growth may be still active at the present day. Carbonates crystallized at 130°C (Dubois et al., 2000) that corresponds more to fluids associated to early generations of quartz. The variations of fluid chemistry and temperature strongly influence the nature of the dissolution-precipitation process and minerals affected.

The relative chronology of fracture fillings is not trivial to define because several fracture and hydrothermal events are superimposed. Outcrop studies on the shoulders of the Upper Rhine Graben shows two successive stages of fillings; a sheared/cataclased phase associated with illite and quartz and a later precipitation of carbonates in tension fractures (Dezayes et al., 2013).

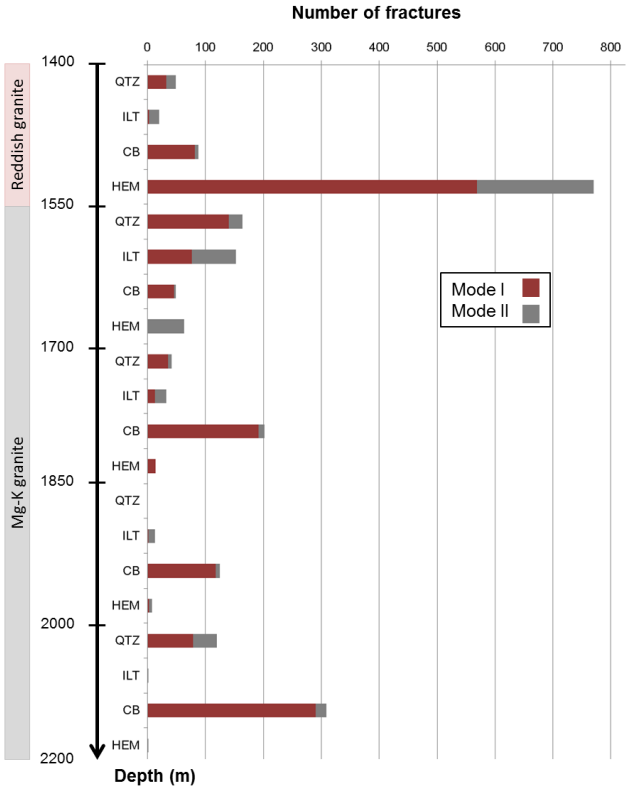

Figure 2 Mineral distribution in fractures of EPS-1 by section of 150-m. Fractures in Mode I and Mode II are differentiated for each mineral.

3. MATERIALS AND METHODS

40 core samples from EPS-1 well located on the first 200 meters of highly altered granite were studied. The results will be described for one sample at 1428m depth. Into the reddish granite matrix (pink), K-felspars are highly microfractured and transformed into illite and primary quartz is visible (Figure 3). A fracture of ~1 cm large is filled by millimetric to micrometric grain-sized minerals, making

difficult their identification only by using optical microscopy. Carbonate (in green) and secondary quartz (in blue) sometimes occur as large grains, but most of them are disseminated as a fine-grained mix with illite, iron oxides and plagioclase relics (brown area).

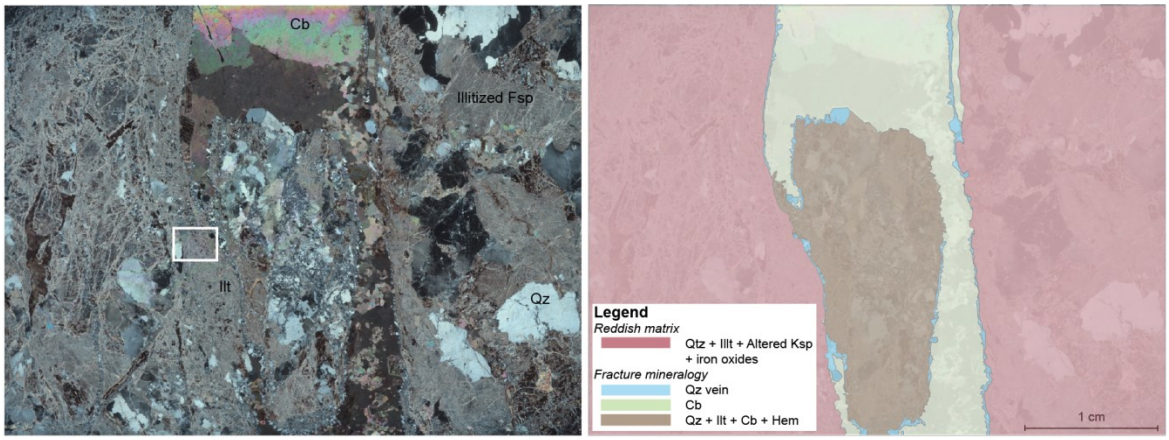

Figure 3 Picture of the thin section studied at the top granitic basement (left) and its schematic representation associated drawing of mineralogy observed microscopically (right). The white frame is the studied zone shown Figure 4.

SEM and electron microprobe analyses were performed at IMPMC (Paris, France) on a 30 µm-thick thin section. SEM analyses were done on a ZEISS ULTRA55 equipped with a FEG-Schottky X-ray source operating at 30 nA with an acceleration voltage of 15 kV. Chemical maps were recorded with a matrix of 1024x758 pixels, a 3 µm step interval in both directions. For each map, the gray scale corresponds to the intensity of the Kα-lines of the different elements (O, Na, Mg, Al, Si, P, S, K, Ca, Ti, Cr, Mn, Fe, Ba, Th, U) calculated from the integration of a specified region of interest (ROI) of the energy range of XRF spectra. Then, ROI maps are used to calculate phase maps thanks to a new routine, specially developed Matlab©-based code, following the same approach than that previously published in Ulrich et al. (2014). The phase map calculation consists first of determining pure mineral phases that are expected to be present in the sample, in order to create standard spectra (or ‘‘pure’’ spectra). Then, for each pixel of the map, a linear combination of the different standard spectra is performed in order to fit each single spectrum. Results provide quantitative phase maps showing the distribution of minerals previously identified in the sample.

A Cameca SX Five electron microprobe was used to determine the major element concentrations of minerals. Operating conditions were 15 kV accelerating voltage, sample current of 30 nA and count time of 3 s/element. Standards used were albite (Na), orthose (K, Al), wollastonite (Mg, Ca and Si), $MnTiO_3$ (Ti and Mn), Cr_2O_3 (Cr), Fe_2O_3 (Fe), P (Apatite), $BaSO_4$ (Ba and S), zircon (Zr), Th (monazite), U (U metal). The analyses have a spatial resolution of 1 micron. The total Fe is presented as FeO.

Trace element analyses in illite were carried out using a LA-ICP-MS at the GeoRessources laboratory (Vandoeuvre-lès-Nancy, France) composed of a 193 nm MicroLas Pro ArF Excimer coupled with the Agilent 7500c quadrupole ICP-MS. Laser ablations were performed with a constant 5 Hz pulse rate, with an ablation crater of 160 µm in diameter. The number of pulses was 200 pulses, sufficient to form a long and stable signal for integration. The ablated material is transported using a constant He flow and mixed with Ar in a cyclone coaxial mixer prior to entering the ICP torch and being ionized. The ions are then sampled, accelerated and focussed before being separated and analysed in the quadrupole mass spectrometer. The following isotopes were monitored: ^{29}Si, ^{39}K, ^{51}V, ^{53}Cr, ^{55}Mn, ^{59}Co, ^{60}Ni, ^{63}Cu, ^{66}Zn, ^{88}Sr, ^{89}Y, ^{137}Ba, ^{232}Th, ^{238}U. Data reduction was carried out using SILLS software (Guillong et al., 2008) and following the standard methods of Longerich et al. (1996), and using Mg content – known from prior EMPA analyses – as an internal standard. External standard calibration was performed with the synthetic glass (NIST 610, Pearce et al., 1997).

In order to compare EPS-1 results to another geothermal well in the Upper Rhine Graben, well-logging data from GRT-1 well at Rittershoffen were analyzed. Only cuttings were available in the well and thus laboratory measurements like in EPS-1 were not possible. Data used for comparison are the spectral gamma ray that measures the natural radioactivity and indicates the variations of U, K and Th content in the well. The large variation of the spectral gamma ray on several meters indicates a variation of granite petrography. A sharp negative variation indicates paleo-circulations into a fractured zone and a leaching of primary magnetic and ferromagnesian minerals. The neutron porosity (NPHI) might be an additional indication of fractured zone if a sharp positive peak correlates with a sharp negative peak of GR. The measurement of neutron porosity is influenced by hydrogen atoms. Thus, the presence of clay minerals highly increases the value of the porosity. Finally, a structural analysis was done from acoustic image logs. Dip value, dip direction, thickness and aperture of fractures were measured on image logs. With structural analysis based on acoustic image logs, the fracture fillings cannot be define and the number and the width of fractures are underestimated compared to structural analysis based on core samples (Genter et al., 1997).

4. RESULTS

4.1 Mineralogy and mineral relations in fracture fillings

Phase maps presented in Figure 4 and Figure 5 focus on the contact between the reddish granite and the fracture fillings and aim to highlight the mineral phase relationship at µm-scale. The mineralogy of fracture fillings includes quartz as large angular clasts (up to 1 mm width and 1.5 mm length) and more diffuse microcrystals (typically on the left-side of the map), albite, illite, carbonates (ankerite

and dolomite) and iron oxides. Illite is ubiquitous, surrounding all other mineral phases. Albite is mainly present as small relics, this mineral being replaced by an assemblage of µ-quartz and carbonates. The close relation between albite, carbonate, and µ-quartz is clearly highlighted in RGB maps (Figure 5a). As illustrated in Figure 5b, dolomite is the dominant carbonate phase. Ankerite only occurs as small grains surrounding large aggregates of dolomite. In addition, both carbonates are systematically associated with small grains of iron oxides.

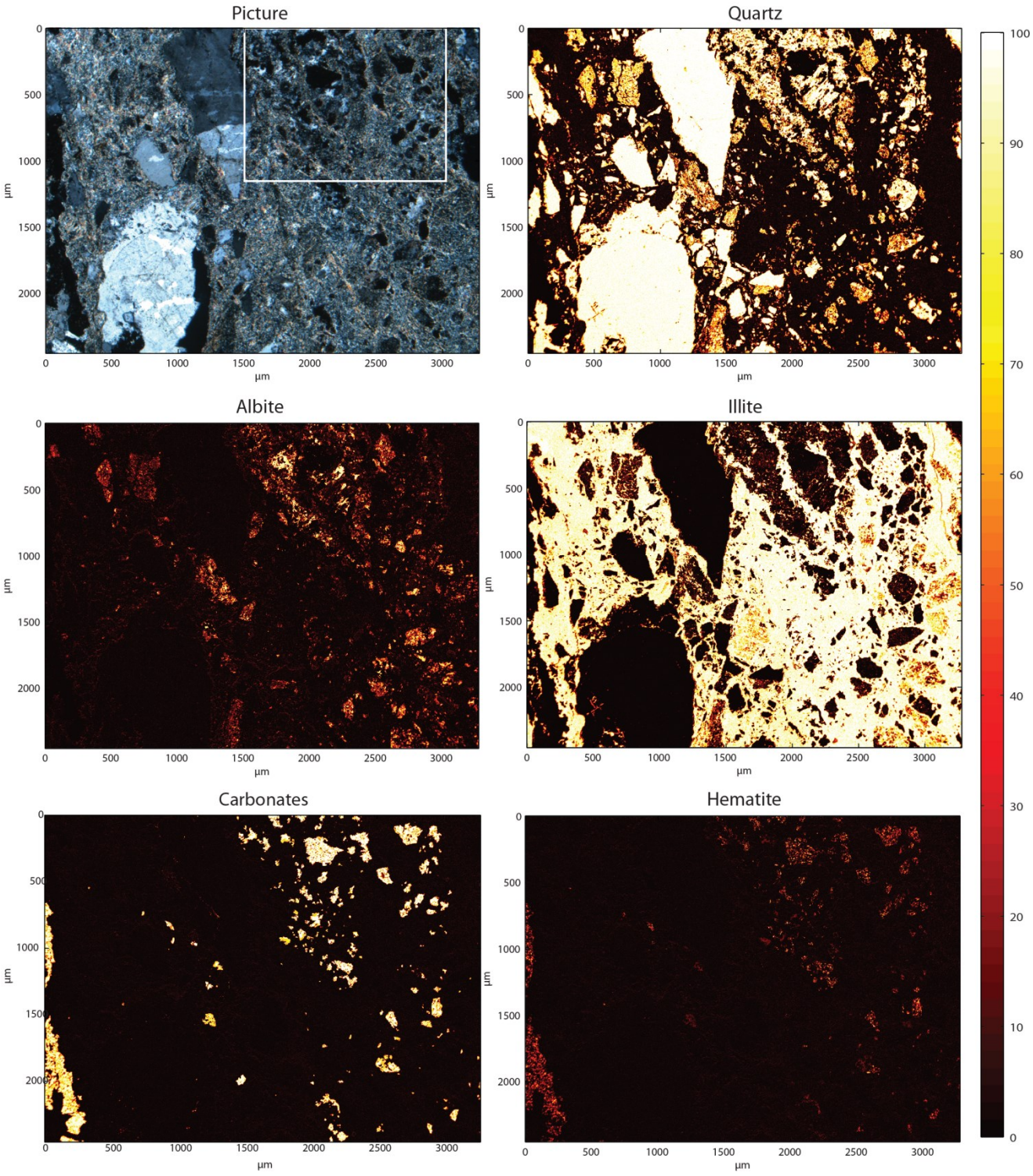

Figure 4 Picture of the focused zone at the edge of the fracture and associated phase mineral maps for quartz, illite, albite, carbonates and iron oxides. The colour bar is in percent of pixel. The white frame on the picture is the zoom into the vein shown Figure 5.

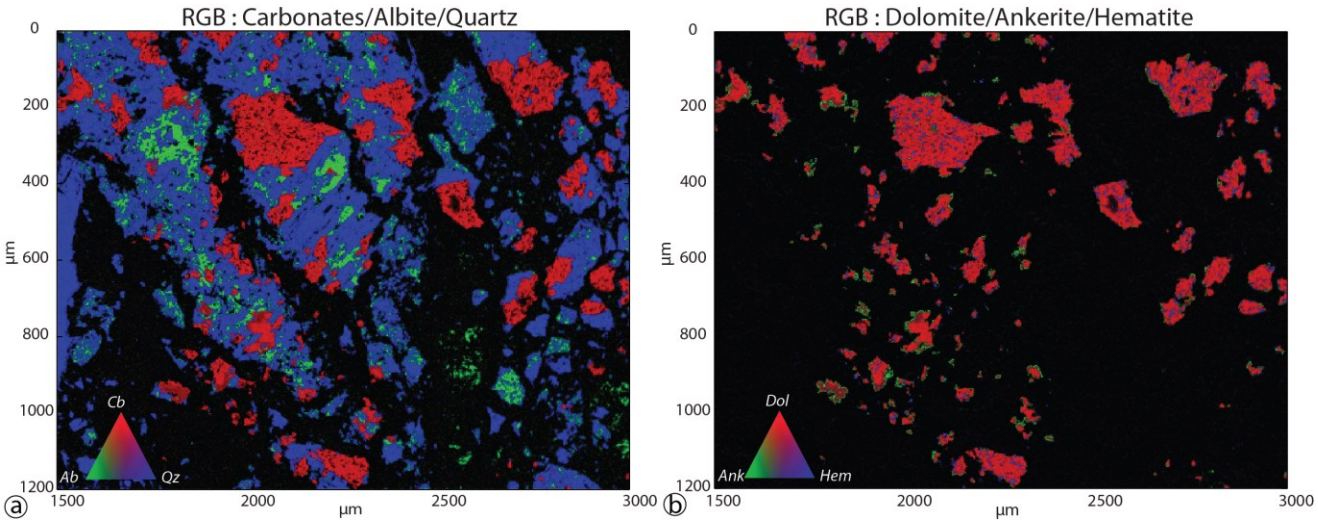

Figure 5 Chemical maps of relationships between carbonates (red), albite (green) and quartz (blue) (left) and between dolomite (red), ankerite (green) and hematite (blue) (rigth) calculated on the basis of SEM measurements into the vein

4.2 Radio-elements distribution

Maps of radio-elements (U and Th) from SEM measurements show that U is mainly hosted by illite. Thus, we performed LA-ICP-MS measurements on illite in order to quantify the amount of radio-elements (Table 1). Results show that U content is in average lower than 0.5 ppm and less than 5 ppm for Th. These concentrations are far below those measured in the granitic basement of the well.

Average Illite												
	SiO_2	TiO_2	Al_2O_3	FeO	MnO	MgO	CaO	Na_2O	K_2O	Cr_2O_3	Total	
wt%	51.57	0.11	30.39	3.40	0.04	2.05	0.41	0.05	8.79	0.03	96.82	
	V	Cr	Co	Ni	Cu	Zn	Sr	Y	Cs	Ba	Th	U
ppm	52.1	2.84	4.90	19.7	6.09	52.7	20.4	0.374	28.6	151	3.50	0.480

Table 1 Average chemical composition of illite analysed by IPC-MS-LA for major and trace elements

4.4 GRT-1 well

In GRT-1 well, temperature gradient has the same shape than in EPS-1 well. The uppermost part of the sedimentary cover is controlled by the conduction regime with a thermal gradient up to 110 K/km. The brittle sediments at the base of the sedimentary cover and the granitic basement are controlled by the convective regime with a thermal gradient lower than 10 K/km. The average GR is 290 gAPI from 2212 to 2259 m depth with an increase of U, Th and K_2O (Figure 6). Below 2259 m depth, the average value of GR decreases to190 gAPI. The rock mass of the top basement, from cuttings description, present a reddish colour and are composed by quartz, illite, K-feldspars and hematite. The porosity measurement does not present significant variations at the top basement with an average value of 2%. The fracture density is about 1.9 fract/m (Vidal et al., 2016).

Below the reddish granite, the GR curve which is highly disturbed, trends with a overall decrease of Th and K_2O content at 2285 m depth (-160 gAPI), 2328 m depth (-180 gAPI) and 2368 m depth (-100 gAPI). These negative anomalies correlate to an increase of the neutron porosity that reaches 35% at 2328 m depth and 23% at 2368 m depth. Natural fractures are systematically filled by various hydrothermal minerals. Their cumulative width with depth presents steps from 1520 to 1860 mm at 2328 m depth, from 1895 to 2740 mm at 2328 m depth and from 3085 to 3455 mm at 2368 m depth (Figure 6). The linear fracture density is about 1.1 fract/m. Corresponding cuttings of this depth section are composed by euhedral quartz, anhydrite, illite and carbonates. Total mud losses were recorded around 2365 m depth during drilling operations.

After 2370 m depth, the GR is more stable with an average value of 260 gAPI and no individual peaks. Cumulative width of fractures does not present major steps and the fracture density is 0.4 fract/m. Mineralogy from cuttings is essentially composed by quartz, biotite, muscovite, K-feldspars, chlorite and illite.

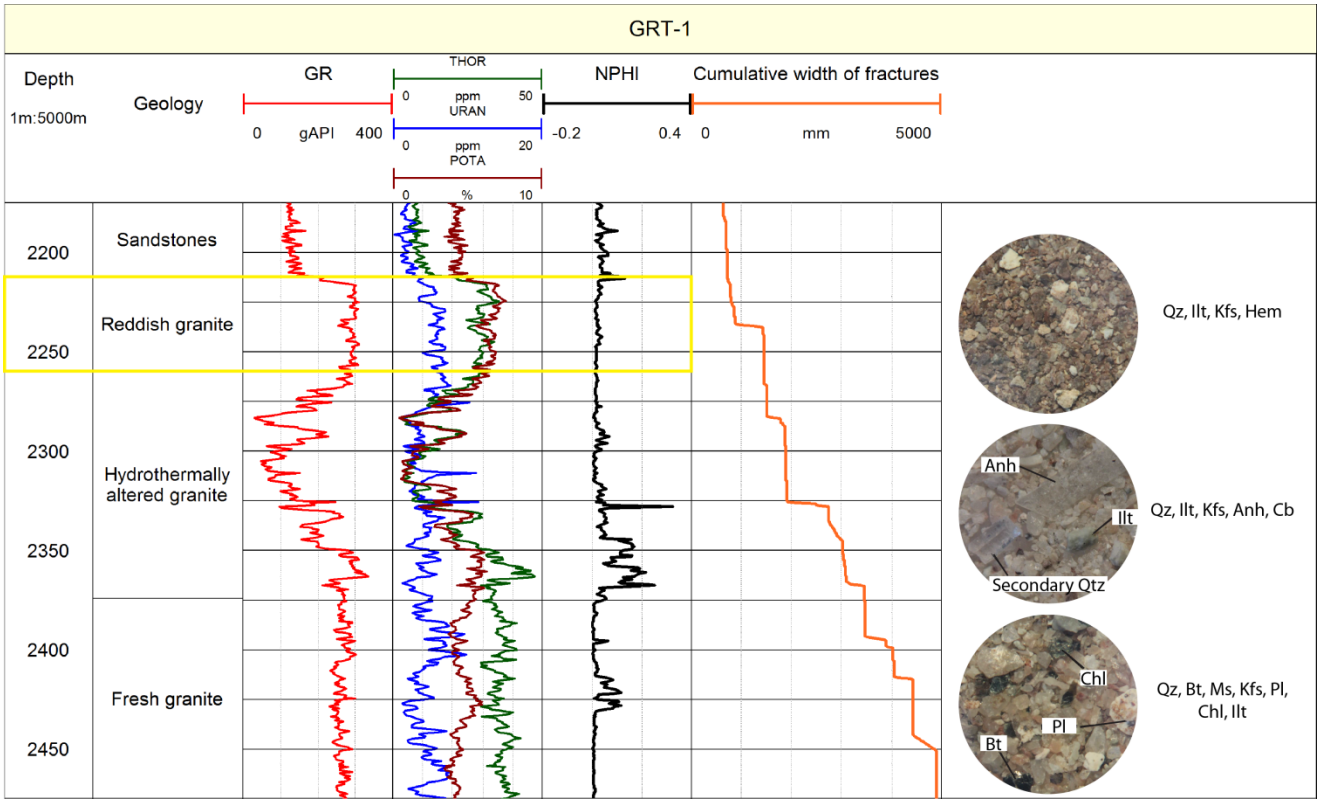

Figure 6 Spectral gamma ray, neutron porosity log and cumulative width of sealed fractures in GRT-& with associated cuttings

5. DISCUSSION

5.1 Dissolution-Precipitation processes and impact on the permeability

On the basis of the mineralogical phase maps and regarding the study of quartz veins by Smith et al. (1998), we infer that there is at least 2 different generations of quartz: Large clasts correspond to the early generation while µ-quartz has crystallized as a consequence of albite imbalance due to fluid circulations. This reaction is accompanied by the precipitation of ankerite: Mg and Fe required to form ankerite are assumed to result from the earlier destabilization of biotite and subsequent chlorite, while Ca results from the alteration of the plagioclase in the deep monzogranite (Aquilina et al., 1997). Ankerite is itself replaced by dolomite, as highlighted by Figure 5b. Reasons for this transition from ankerite to dolomite remain unclear. However RGB maps show that this reaction is accompanied by the release of iron that precipitates into hematite. Simultaneous precipitations of dolomite, which occurs in reducing conditions, and hematite, which supposes oxidizing conditions, indicate that changes of redox conditions may occur at grain scale. Finally, illite map indicate that this clay mineral has precipitated directly from the fluid, plugging the system (Figure 4). The precipitation of illite probably prevents further fluid circulations and thus stopes all processes of dissolution-precipitation previously described.

At the fracture scale, carbonates and quartz veins are the last minerals to precipitate (Figure 3). These preliminary results show that each reaction associated to successive hydrothermal events form secondary minerals characterized by higher molar volume than the primary ones. This significant gain of volume reduces the connected porosity and consequently the fracture permeability.

At the basement scale, the neutron porosity measurements in the well also indicate a decrease of the porosity at the top basement (Figure 6). Some fractured zones are observed from well-logging variations in the underlying altered granite. They may be sealed at the borehole scale acting as a barrier for fluid circulation. Alternatively, they may present a residual permeability and be connected to a larger fracture network through the granitic basement.

5.2 Conceptual model

The early stage of alteration is pervasive, when plagioclase is altered into corrensite and biotite into chlorite during the granite batholith emplacement. The quartz remains stable. Then successive hydrothermal alterations correlated to tectonic and fracturing events through the geological history of this area. In both fractured zones and matrix, corrensite and chlorite are transformed into illite, which is also the case for K-feldspars when shearing occurs. Secondary quartz and carbonates precipitate into fractured zones. Paleo-emersion of the top of the granite leads to a decompression involving nearly horizontal jointing and a subsequent episode of paleo-weathering. Ankerite is replaced by dolomite and hematite crystallise at the edge of carbonates. Finally, subsidence related to the extension of the Upper Rhine Graben causes the burying of the granitic basement under a stack of thick sediments. Mesozoic and Cenozoic tectonic events such as reactivation of Hercynian structures and creation of new one affect the granitic basement. The P-T conditions increase to reach modern temperature and pressure conditions. During post-Variscan events, the mineral transformations such as ankerite destabilisation to dolomite continue until illite precipitation plugs the system. Quartz and carbonates crystallise into fractured zone as veins. Quartz is

the only mineral considered as actively growing. The chain reaction of dissolution-precipitation processes lead to reduce the connected porosity. Fractures that are critically stressed might present residual permeability (Evans et al., 2005).

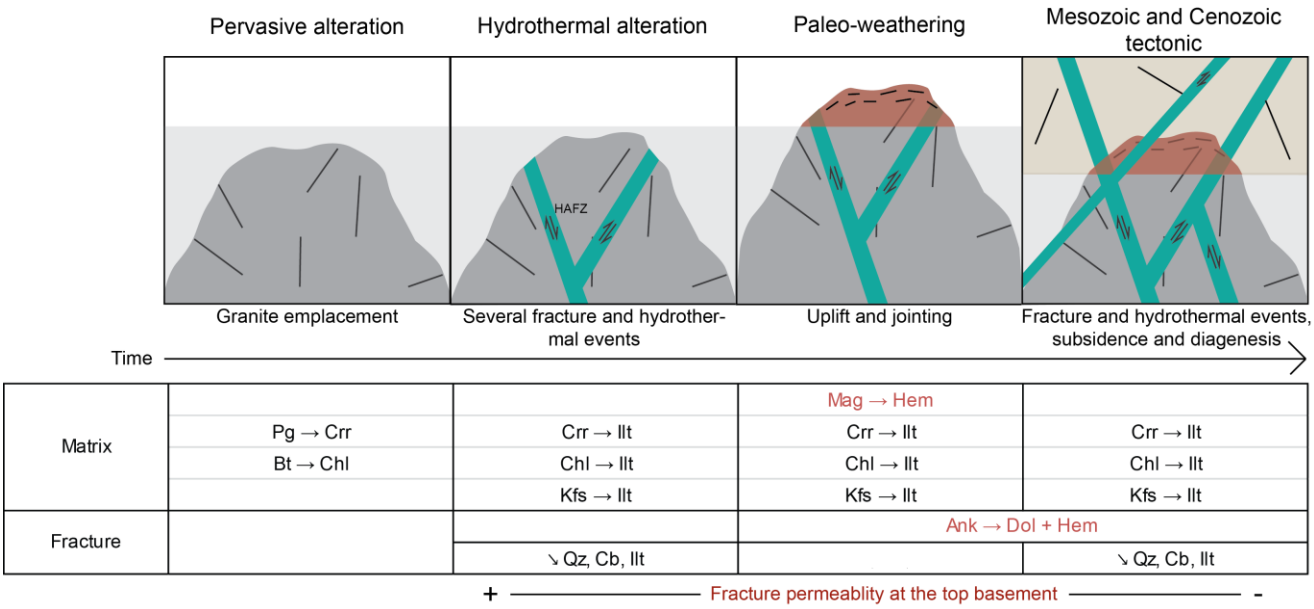

Figure 7 Conceptual model of alteration and mineral transformation of hidden granite in geothermal granite. Specific mineral transformations observed at the top basement are indicated in red.

6. CONCLUSION

In conclusion, fractures mineralogy in the reddish granite were analysed by several laboratory methods. Results reveal complex zone into the fracture where precipitation of secondary quartz and ankerite takes place. These precipitations are assumed to occur after albite destabilisation reacting with Mg- Fe- and Ca-rich fluid circulating through deep granite. Ankerite, dolomite and hematite are closely associated and suggest ankerite replacement by dolomite accompanied by the release of iron that precipitates into hematite. The precipitation of illite probably prevents further fluid circulations and thus all processes of dissolution-precipitation. Carbonates are also observed around complex zones into the fracture with quartz vein crystallising at the edge. Successive precipitations of secondary minerals associated to hydrothermal events and fluid circulation decrease the fracture permeability. The lower porosity of the reddish granite is correlated to an increase of the natural radioactivity observed in several geothermal well of the Northern Upper Rhine Graben thanks to well-logging data. The preliminary results do not allow defining which mineral bears radio-elements that are concentrated into the reddish granite located at the top basement.

ACKNOWLEDGMENTS

The authors are grateful to the GEIE Exploitation Minière de la Chaleur for providing Soultz core samples and geophysical data and ECOGI company for the Rittershoffen geophysical logs. A part of this work was done in the framework of the LabEx G-Eau-Thermie Profonde which is co-funded by the French government under the program “Investissements d’Avenir”. The extended abstract was performed as a contribution to the PhD thesis of Jeanne Vidal co-founded by ADEME (French Agency for Environment and Energy). The authors thank M. Amann and O. Boudouma for helping during laboratory analysis.

REFERENCES

Aquilina, L., Pauwels, H., Genter, A., and Fouillac, C.: Water-rock interaction processes in the Triassic sandstone and the granitic basement of the Rhine Graben: Geochimical investigation of a geothermal reservoir, *Geochim. et Cosmochim. Acta*, **61**, (1997), 4281-4295.

Cocherie, A., Guerrot, C., Fannin, C.M., and Genter, A.: Datation U–Pb des deux faciès du granite de Soultz (Fossé rhénan, France), *C. R. Geoscience*, **336**, (2004), 775-787.

Dezayes, C., Lerouge, C., Ramboz, C., and Wille G.: Relative chronology of deep circulations within the fractured basement of the Upper Rhine Graben, *Proceedings*, European Geothermal Congress, Pisa, Italy (2103).

Dubois, M, Ledésert, B, Potdevin, J.L, and Vançon, S.: Détermination des conditions de précipitation des carbonates dans une zone d’altération du granite de Soultz (soubassement du fossé Rhénan, France): l’enregistrement des inclusions fluides, *C. R. Acad. Sci. Paris*, **331**, (2000), 303–309.

Evans, K.E., Genter, A;, and Sausse, J.: Permeability creation and damage due to massive fluid injections into granite at 3.5 km at Soultz, *J Geophys Res*, **110**, (2005).

Genter, A.: Géothermie roches chaudes sèches: le granite de Soultz-sous-Forêts (Bas-Rhin, France). Fracturation naturelle, altérations hydrothermales et interaction eau-roche., *PhD thesis*, University of Orléans, France (1989).

Genter, A., and Traineau, H: Analysis of macroscopic fractures in granite in the HDR geothermal well EPS-1, Soultz-sous-Forêts, France, *J Volcanol Geotherm Res*, **72**, (1996), 121–141.

Genter, A., Castaing, C., Dezayes, C., Tenzer, H., Traineau, H., Villemin, T: Comparative analysis of direct (core) and indirect (borehole imaging tools) collection of fracture data in the Hot Dry Rock Soultz reservoir (France), *J Geophys Res* **102**(B7), (1997), 15,419–15,431.

Guillong, M., Meier, D.L., Allan, M.M., Heinrich, C.A., and Yardley, B.W.: Appendix A6: SILLS: a MatLab-based program for the reduction of Laser Ablation ICP-MS data of homogeneous materials and inclusions, *Mineralogical Association of Canada Short Course* **40**, (2008), 328–333.

Longerich, H.P., Jackson, S.E., and Günther, D.: Laser ablation inductively coupled plasma mass spectrometric transient signal data acquisition and analyte concentration calculation, *Journal of Analytical Atomic Spectrometry,* **11**, (1996), 899–904.

Pearce, N.J.G., Perkins, W.T., Westgate, J.A., Gorton, M.P., Jackson, S.E., Neal, C.R., and Chenery, S.P.: A Compilation of New and Published Major and Trace Element Data for NIST SRM 610 and NIST SRM 612 Glass Reference Materials. *Geostandards and Geoanalytical Research*, **21**, (1997), 115–144.

Schellschmidt, R., and Clauser, C.: The thermal regime of the Upper Rhine Graben and the anomaly at Soultz, *Z Angew Geol*, **12**, (1996), 40–44.

Schleicher, A.M., Warr, L.N., Kober, B., Laverret, A., and Clauer, N.: Episodic mineralization of hydrothermal illite in Soultz-sous-Forêts granite (Upper Rhine Graben, France), *Contrib Mineral Petrol*, **152**, (2006), 349-364.

Smith, M.P., Savary, V., Yardley, B.W.D., Valley, J.W., Royer, J.J., and Dubois, M.: The evolution of the deep flow regime at Soultz-sous-Forfts, Rhine Graben, eastern France: Evidence from a composite quartz vein, *J Geophys Res*, **103**(B11), (1998), 223-237

Stussi, J.M., Cheilletz, A., Royer, J.J., Chèvremont, P., and Gilbert, F.: The hidden monzogranite of Soultz-sous-Forêts (RhineGraben, France), mineralogy, petrology and genesis, *Géol Fr*, **1**, (2002), 45–64

Pribnow, D., and Schellschmidt, R.: Thermal tracking of upper crustal fluid flow in the Rhine Graben, *Geophysical Research Letters*, **27,** (2000).

Ulrich, M., Munoz, M., Guillot, S., Cathelineau, M., Picard, C., Quesnel, B., Boulvais, P., and Couteau, C.: Dissolution–precipitation processes governing the carbonation and silicification of the serpentinite sole of the New Caledonia ophiolite, *Contrib Mineral Petrol* **167**, (2014), 952-19.

Vidal, J., Genter, A., Schmittbuhl, J., Baujard, C., and Dalmais, E.: Natural fractures and permeability at the geothermal site Rittershoffen, France, *Proceedings*, European Geothermal Congress, Strasbourg, France (2106).